sciendo

CIVIL AND ENVIRONMENTAL ENGINEERING REPORTS

E-ISSN 2450-8594

CEER 2020; 30 (1): 087-110
DOI: 10.2478/ceer-2020-0008
Original Research Article

RELIABILITY-BASED SAFETY EVALUATION OF THE BISTOON HISTORIC MASONRY ARCH BRIDGE

Majid POURAMINIAN[1], Somayyeh POURBAKHSHIAN[1], Ehsan NOROOZINEJAD FARSANGI[2*], Sevil BERENJI[3], Salman KEYANI BORUJENI[4], Mirhasan MOOSAVI ASL[5], Mehdi MOHAMMAD HOSSEINI[1]

[1] Department of Civil Engineering, Ramsar Branch, Islamic Azad University, Ramsar, Iran
[2] Faculty of Civil and Surveying Engineering, Graduate University of Advanced Technology, Kerman, Iran
[3] School of Environment, Enterprise and Development (SEED), University of Waterloo, Waterloo, Canada
[4] Department of Civil and Environmental Engineering, Politecnico di Milano, Lecco, Italy
[5] Department of Civil Engineering, Salmas Branch, Islamic Azad University, Salmas, Iran

Abstract

This research examines the probabilistic safety assessment of the historic BISTOON arch bridge. Probabilistic analysis based on the Load-Resistance model was performed. The evaluation of implicit functions of load and resistance was performed by the finite element method, and the Monte-Carlo approach was used for experiment simulation. The sampling method used was Latin Hypercube. Four random variables were considered including modulus of elasticity of brick and infilled materials and the specific mass of brick and infilled materials. The normal distribution was used to express the statistical properties of the random variables. The coefficient of variation was defined as 10%. Linear behavior was assumed for the bridge materials. Three output parameters of maximum bridge displacement, maximum tensile stress, and minimum compressive stress were assigned as structural limit states. A sensitivity analysis for probabilistic

[*] Corresponding author: Graduate University of Advanced Technology, Assistant Professor Ehsan Noroozinejad Farsangi, e-mail: noroozinejad@kgut.ac.ir

analysis was performed using the Spearman ranking method. The results showed that the sensitivity of output parameters to infilled density changes is high. The results also indicated that the system probability of failure is equal to $p_f^{system} = 1.55 \times 10^{-3}$. The bridge safety index value obtained is $\beta^t = 2.96$, which is lower than the recommended target safety index. The required safety parameters for the bridge have not been met and the bridge is at the risk of failure.

Keywords: masonry arch bridge, probability of failure, epistemic uncertainty, sensitivity analysis, Monte Carlo simulation

1. INTRODUCTION

Historical structures in any country indicate their antiquity and history and are considered as symbols of the cultural heritage of the country, therefore, they must be preserved and protected. During the process of constructing these structures, the gravitational and lateral loads were not necessarily estimated accurately; hence, scrutiny of their vulnerability is a must and, if required, work to retrofit, restore or renovate them must be carried out. Cultural heritage structures are considered to be high-importance-structures and their structural behavior should be analyzed carefully and precisely. These structures, because of their geometrical complexities and conventional eroded materials, cannot easily be modeled accurately and precisely. Moreover, due to international restrictions, they cannot be tested with known destructive tests. Researchers have utilized different testing methods to explore the physical and mechanical properties of masonry materials to discover the damage to the internal parts of structures in which there is no proper access, including non-destructive-tests or semi-destructive-tests. One of the most important characteristics to evaluate the strength of historical structures is the estimation of the compressive strength of masonry materials. In this research [1,11,12,13,16,27,32,39] the Schmidt-Hammer-Test, Ultrasonic pulse velocity, compressive jack test from core drilling samples, and the in-situ drilling resistance technique have been utilized to estimate the compressive strength. Valluzzi et al. used Infrared Thermography and ambient vibration tests to assess the structural qualification of the Sarno Baths, Pompeii [40]. Altunişik et al. performed experimental measurements by ambient vibration test on an ancient masonry Bastion and extracted three first natural frequencies of the Bastion [3]. Many studies were done on the structural behavior assessment of historic monumental construction by finite element modeling and analysis [4,6,7,9,14,15,17-19,22,24,25,28,29,31,35,38]. Micic et al. (2015) studied the probabilistic analysis of the strength of masonry building walls over time. They modeled a macro sample of the wall in the FEM software

of ANSYS and, for the stochastic modeling, performed the Monte-Carlo simulation by the Latin-Hypercube sampling method. The considered probabilistic inputs during their research included the dimension of the wall, the loads, and the strength of the materials. The vertical deformation and the Von-Mises Tensions were calculated by Limit State Functions. The sensitivity of the response of the structure to the probabilistic variables was also performed [26]. Hardil et al. (2001) analyzed the stochastic finite elements of historical masonry bridges considering operational loads and temperature. Evaluation of the safety of the Námešt nad Oslavou Bridge was studied by considering uncertainties in order to retrofit and renovate the bridge [20]. The results suggested that retrofitting the bridge without performing a meticulous study of its properties would lead to a decrease in the safety of the bridge with respect to its initial condition, one of the main reasons being retrofitting the passage of the bridge with concrete. The result of this research was that the probabilistic analysis gives huge structural responses to the analyzer that help the decision-making process when selecting the proper retrofitting method, with a higher level of trustworthiness. Reliability-based assessment of vault bridges on the serviceability limit states and ultimate limit states was performed by Casas et al. (2011) [10]. After assessing the results of failure modes from laboratory results, masonry vaults were introduced. Due to a lack of response model and reliable information about the materials, the study was only performed on the four-hinge-mechanism and the ring-separation. The possibility of fatigue-rupture of the masonry bridge under serviceability loads and also estimations based on the reliability of the bridge for the limit state of the four hinges were studied. The bridge was loaded for the fatigue evaluation under safe conditions and sensitivity analysis to investigate the safety of the bridge, due to the reduction of the compressive strength of the bricks on one of the columns under the erosion of the materials, was also studied. Pouraminian et al. (2019) studied the reliability analysis of a masonry-arch-bridge under serviceability loads. Uncertainties are produced by the probabilistic platform in ANSYS software and are controlled in each safety structural cycle. A failure-tree is given for the arch-bridge system and it is assumed that the failure of the bridge-system is due to the failure of three components being rupture in tension, rupture in compression, and over-allowable span-rise. These three components are assumed to be in a sequence where failure in each of them leads to the failure of the entire bridge system. Sensitivity analysis for the limit functions of stochastic variables was also performed. It was determined that the maximum compression occurred with the variation of the Young Modulus of the bridge-vault. The maximum tension, however, occurred for the variation of the Young Modulus of the bridge-passage, and the maximum deformation occurred with respect to the variation of the specific-mass of the lateral walls of the bridge [34]. In numerous studies, the

PDS has been used to evaluate the reliability of structures [6,33,34,37]. The PDS tool of ANSYS software is used for sensitivity analysis and to calculate the probability of failure.

The main aim of this paper is to evaluate the probabilistic safety of a historical masonry bridge using a stochastic finite element method. The safety index has been used to determine the safety status of this heritage construction. A case study for this paper is the construction of the BISTOON historical masonry arch bridge in the north-west of Iran.

2. BISTOON BRIDGE

Bistoon Bridge is located in the east part of Bistoon city on the Sahneh to Kermanshah highway in the Dinevar-Ab river region. This bridge is located on the road which connected the cities of Qazvin and Hamedan, following the cities of Kermanshah and Baghdad during the Safavids-Dynasty. The bridge construction probably dates back to the reign of King-Abbas-I, however, its piers and foundations were probably constructed earlier during the Sasanian-Empire, due to the Sasanian symbols engraved on its surfaces, although the construction was not completed due to unknown reasons. In the Hasanwayhids-era (961-1015 A.D), the bridge was completed and in the Ilkhanate-Dynasty (1219-24 A.D), the fourth span of the bridge, along with the triangular piers, was restored. The façade was rebuilt during the Safavids-dynasty. Furthermore, a brick kiln was constructed on the north-west side of the bridge within its reconstruction program. During the first Pahlavi era, the third arch of the bridge and the façade were restored to their original shape. Although many restorations have been carried out since that time by the Cultural and Heritage Organization of Kermanshah Province, the bridge is about to collapse completely and be demolished.

This bridge has a length of 115 m and a width of 6.90 m including its parapet. The width of each parapet wall is 37 cm and its height from the bridge pavement level is 50 cm. All the parapet walls except for a small section of about 8.40 m in length, located on the south-western part of the bridge, have been destroyed over time. This bridge has been built in an east-west direction and consists of 4 unequal spans. The piers, except for the side piers, are hexagonal and have been built using rubble, gravel, and lime-mortar with their surface covered with scraped rectangular stones. The middle section of the piers is rectangular and forms the basic part of the pier. The bridge piers have been constructed using scraped stones to a height of 3.55 m. There are triangular cutwaters in both sides of the piers with 4.65 m on its isosceles triangle side and above them, the piers are in prismatic form. Arches are constructed of brick (28×27×7 cm,

22.5×21.5×5.5 cm, and 24×24×5 cm in a Roman arch) and lime-mortar, and the bridge carriageway is constructed of river rubble stone and lime-mortar to produce a cobblestone pavement. There are two small and two large bridge spans. The spans of the arches from east to west are 5.00 m, 4.90 m, 11.00 m, and 11.50 m and their heights are 6.50 m, 6.22 m, 10.50 m, and 9.50 m from the riverbed, respectively. The arch types from east to west are sharp lancet arches (Sharp five to seven lancet arch), mild lancet arches (Mild five to seven lancet arch), Roman arches (Halochin) in which the cross-section geometry of this arch is something between elliptical and circular due to some reconstruction programs in its history, after its demolition which changed its lancet arch to a Roman arch, and mild lancet (Mild five to seven lancet arch) type, respectively. The arches of Bistoon Bridge are, therefore, lancet arches except for one which was changed to a Roman arch. They are mostly used in large spans with a high span to rise ratio and were applied mostly to spans over 4.16 m and lower than 16.64 m. However, in Roman arches, the extremely high span to rise ratio in large spans is not applicable and strong materials should be used. In Mild five to seven lancet arches, spans tolerate distances of between 3.12 m to 4.16 m.

The most significant difference of this bridge compared to other bridges in the region is in the construction of its arches; the largest face of the bricks was placed towards the outer part of the arch, whereas, the other bridges have the smallest sides of the bricks facing outward.

Figure 1 shows the image of the Bistoon-bridge from downstream. According to the valid evidence and available documents, the columns of the Bistoon bridge were constructed in the late Sasanid-Dynasty and, similar to most other structures of that era, have not been completed. In the 4th century A.D., the local governors completed the bridge and from those constructions, solely two vaults from the total of four and the circular retaining walls remain. The mid-section has a rectangular shape which on both sides of this cube is in the same direction as the water current, with triangular gutters. On the northern and southern views of the bridge, on each of the gutters, are triangular or circular retainers made from brick that play an important role in preventing the vaults from drifting. The columns of the bridge were made of stone and plaster mortar and covered with curved rectangular stones, while the inner parts were made from pebble, rubble, and plaster mortar. The vaults of the bridge were made of brick with plaster mortar and the passage over the bridge was made of plaster mortar and pebbles. The biggest vault is on the most western part.

Fig. 1. Photograph of the Historic BISTOON Masonry Arch Bridge in Iran

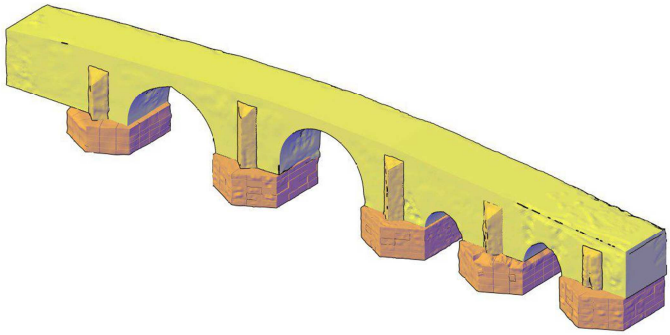

Fig. 2. Isometric images of the BISTOON bridge

3. EXPERIMENTAL TESTS

In this research, a total number of 13 clay bricks with complete dimensions were tested. The tested clay brick specimens are shown in Figure 3. Firstly, they were dried in an oven, then their dimensions were measured with calipers, after which their specific weight was calculated, and the compressive strength of the samples was determined by a uniaxial pressure test. The histogram of the geometrical and strength data distribution for the performed tests on the clay brick specimens is

shown in Figure 4. The mean value for the compressive uniaxial strength and the standard deviation of the brick samples are $f_b^{mean} = 10.78MPa$ and $\sigma_{fb} = 1.72MPa$, respectively. Regarding the looseness of the masonry-mortar and its inaccessibility, this was hypothesized as $f_m = 1MPa$. A Freezing-Test was performed on the brick samples with 50 freeze/thaw cycles and, as a result, a weight loss of 1.1 to 8.6 percent was observed.

To determine the compressive strength of the masonry-materials in the macro-model, Equations of (3.1) and (3.2) were applied [8]. The authors utilized Equation (3.2) for safety reasoning. The *n* parameter is assumed as 1. The allowable compressive strength $f_k = 1.8MPa$ was applied in the finite element software as the compressive strength of homogenous masonry materials (Brick-mortar).

$$f_k = K * f_b^{0.7} * f_m^{0.3} (MPa) \tag{3.1}$$

$$f_b = f_b^{mean} - n * \sigma_{fb} \tag{3.2}$$

Fig. 3. Test specimens

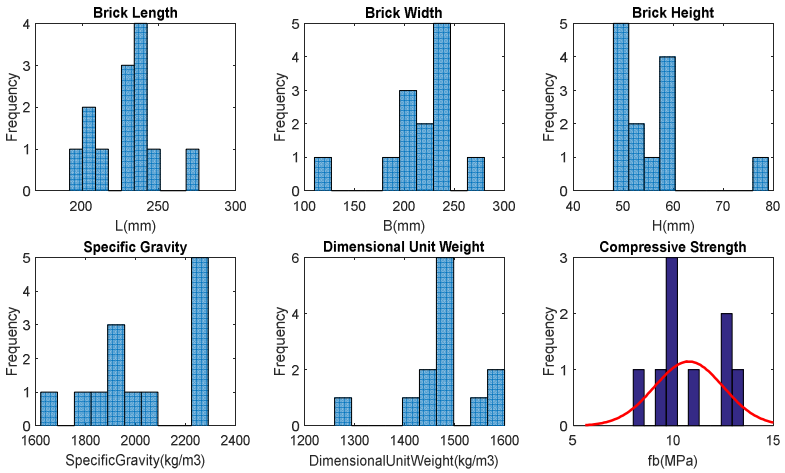

Fig. 4. Geometrical and strength data distribution for clay brick specimens

4. DETERMINISTIC AND PROBABILISTIC FE

The ANSYS popular finite element software was used to analyze the BISTOON bridge. Many civil engineering field studies have used ANSYS software for analysis of structures [6,33,35-38]. To assess the safety level of the bridge, probabilistic analysis based on the Load-Resistance model is utilized, as in many previous studies to assess the probabilistic safety of civil engineering structures [6,21,33,34]. To perform the probabilistic analysis of the BISTOON arch bridge, it is necessary to define our random variables in advance. To define random variables, we can use the given data in the technical literature and/or from laboratory observations. The specific mass of the materials in the body of the bridge (Bridge own weight) and the traffic loads are the loads that are imposed on the bridge structure. Also, the properties of the strength of the bridge are mainly the modulus of elasticity, the specific mass of the filler-materials, the formation of the arches, and the lateral walls. In Figure 5, the applied stochastic finite element model is shown. The physical properties of the masonry materials, including the modulus of elasticity and the specific mass, are generated randomly.

4.1. Discretizational model

For the materials of the bridge, linear behavior has been considered. In modeling the body of the masonry bridge, the strategy of macro-modeling and homogeneity of the mechanical properties of materials in different directions is used. In Figure 5, the discretized model that has been applied in FEM is shown.

3-Dimensional SOLID185 isoparametric-elements with eight nodes were used such that each node has three degrees-of-freedom. The number of the elements and nodes for the discretized model are 11012 and 14538 respectively. On the supports of the bridge, where the bridge is connected to the bed-rock of the river, the boundary conditions were considered as rigid. The mechanical and physical properties of the materials are applied based on the performed tests and the advice of the technical literature. For the materials of the vaults and the lateral walls, the modulus of elasticity is $E_B = 2.2GPa$, the Poisson ratio is $\nu_B = 0.2$, and the density of concrete is considered as $\rho_B = 1800 {kg}/{m^3}$ for the physical properties in the FE modeling. Moreover, for the infilled materials and the deck passage over the bridge, the modulus of elasticity is $E_{Infilled} = 0.2GPa$, the Poisson ratio is $\nu_{Infilled} = 0.22$, and the density of concrete is considered as $\rho_{Infilled} = 2000 {kg}/{m^3}$ (The mean values are given in Table 1).

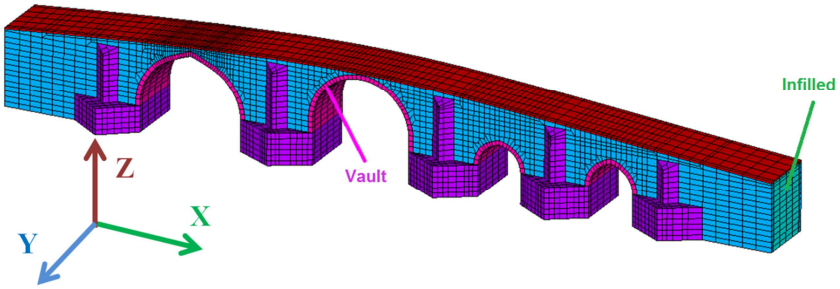

Fig. 5. Discretization of the finite element model

4.2. Deterministic static analysis

After implementing the bridge in the ANSYS FE platform, it was analyzed under the gravitational and the traffic loads $300 {dN}/{m^2}$. The bridge structure was analyzed statically. Minimum principal stress, maximum principal stress, and the maximum deflection of the bridge span are utilized as the strength control in compression, tension, and operational controls, respectively. The distribution of the tensile and compressive stresses and the deformation are shown in Figures 6 to 8, respectively. Under the aforementioned loading, the maximum of the principal stress will be $S1^{\max} = 0.65MPa$ and the minimum of the principal stress will be $S3^{\min} = -0.92MPa$, the maximum deformation will be $D^{\max} = 2.79mm$, and except for the tensile stress, all the other values are less than their allowed values, i.e. $S1^{allow} = 0.15MPa$, $S3^{allow} = -1.8MPa$, and

$D^{allow} = 5.75mm$. The allowed values of BISTOON bridge deflection are assumed to be $D^{allow} = \frac{S}{2000}(cm)$, where S=1150cm is the length of the arch span [34].

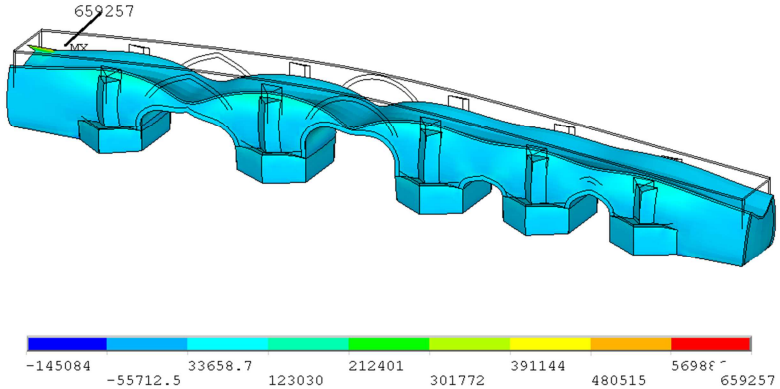

Fig. 6. The maximum of the tensile stress under gravitational loading [Pa]

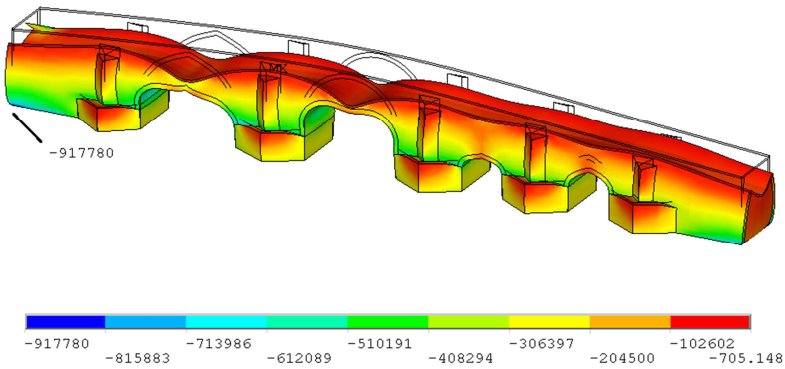

Fig. 7. The minimum principal stress under gravitational loading [Pa]

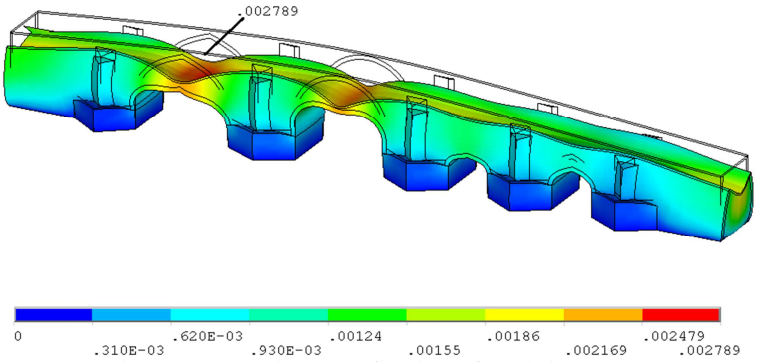

Fig. 8. The maximum deflection of the bridge [m]

4.3. Deterministic modal analysis

After the free vibration analysis, the first three vibrational frequency modes with the damping ratio $\xi = 5\%$ would be according to Figure 9., i.e. $f_1 = 5.48Hz$, $f_2 = 5.86Hz$, and $f_3 = 6.25Hz$. The Block Lanczos method was used for the mode extraction.

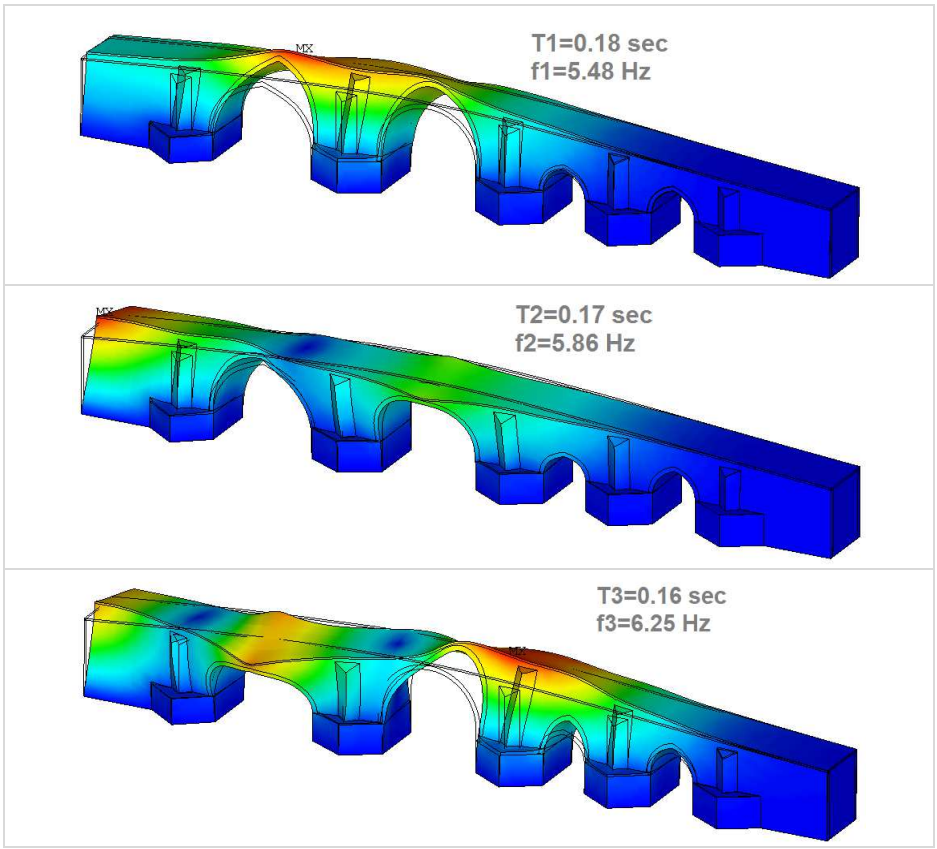

Fig. 9. First Three Modal Shapes of The BISTOON bridges

4.4. Random variables

Four random parameters were considered in probabilistic analysis. These random parameters are defined by the Gaussian probability density function (PDF) shape. In Table 1, the type of variables, PDF, mean value, and standard deviation are also shown. The values in the table are selected according to technical literature.

Table 1. Random variables defined in the finite element model of Bistoon Bridge

Random Parameters	**Index**	**Unit**	**Dist.**	**Mean** (μ)	**Standard deviation** (σ)
Elasticity Modulus of Bricks	E_B	GPa	N	2.2	0.22
Density of Bricks	ρ_B	kg/m^3	N	1800	180
Elasticity Modulus of Infilled	$E_{infilled}$	GPa	N	0.2	0.02
Density of Infilled	$\rho_{Infilled}$	kg/m^3	N	2000	200

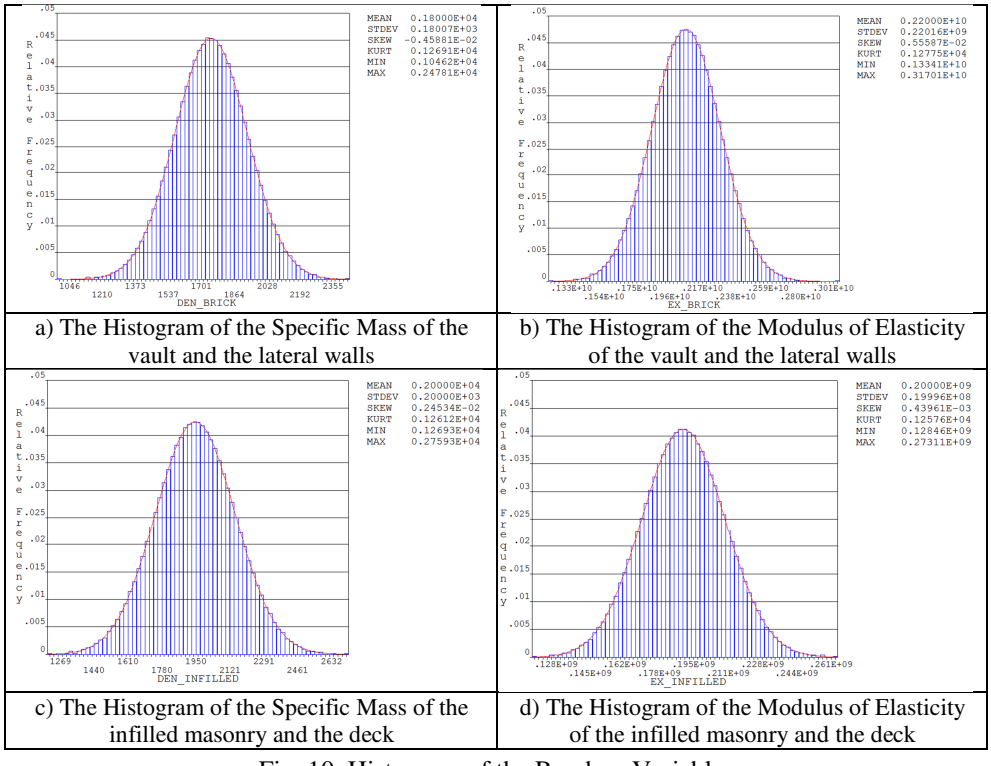

a) The Histogram of the Specific Mass of the vault and the lateral walls

b) The Histogram of the Modulus of Elasticity of the vault and the lateral walls

c) The Histogram of the Specific Mass of the infilled masonry and the deck

d) The Histogram of the Modulus of Elasticity of the infilled masonry and the deck

Fig. 10. Histogram of the Random Variables

By utilizing the Monte-Carlo simulation method and Latin hypercube Sampling, 5000 simulated samples have been produced that are shown in Figure 10. In Figure 10(a), the histogram of the specific mass of the masonry materials of the vaults and the lateral walls are shown with a mean value of $1800\,kg/m^3$ and a standard deviation of $180\,kg/m^3$. In Figure 10(b), the histogram of the modulus of elasticity of the materials of the vaults and the lateral walls are shown with a mean-value of 2.2GPa and a standard deviation of 0.22GPa. In Figure 10(c), the

histogram of the specific mass of the masonry materials and the top-passageway are shown with a mean value of 2000 kg/m^3 and a standard deviation of 200 kg/m^3. In Figure10(d), the histogram of the modulus of elasticity of the masonry fillers and the top-passageway is shown with a mean value of 0.2 GPa and a standard deviation of 0.02 GPa.

4.5. Histogram of output parameters

To determine the histogram of the failure function, rather than producing random data, there is a need to calculate output parameters $(S1_{Allow}; S3_{Allow}; D_{Allow})$ in every simulation with finite element analysis. On the left side of Figure 11, histograms of the output parameters for the maximum deflection, maximum tensile stress, and minimum compressive stress for all the simulation loops produced by MCS are shown. Statistical properties of the output parameters are shown, including the mean value, standard deviation, etc. On the right side of Figure 11, the histogram of 5000 simulation loops of the failure function for the three aforementioned limit states is shown. The negative values of the failure functions $GF_{LS}(X) \prec 0$ indicate the risk of exceedance from special limit states and induced damage to the bridge.

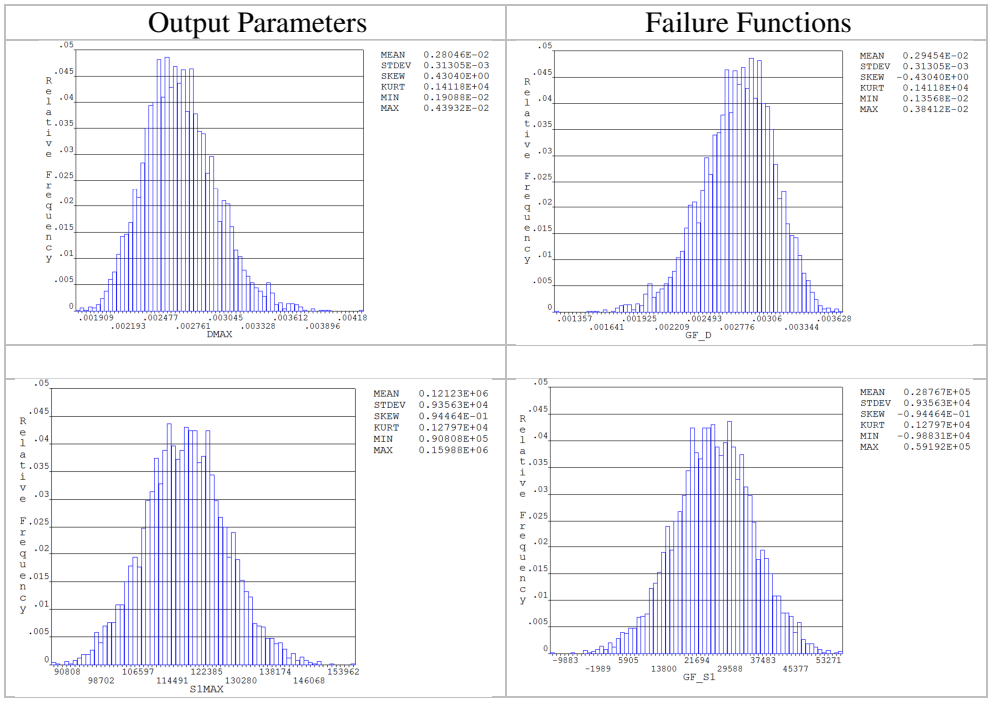

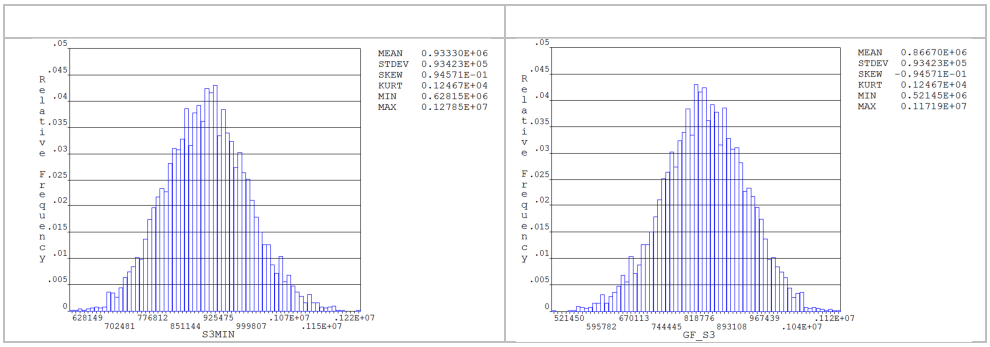

Fig. 11. Histogram of the output parameters: maximum deflection, maximum tensile stress, and minimum compressive stress of the bridge materials

4.6. Probabilistic analysis

To accelerate the assessment of the values of the failure functions, the Monte-Carlo Latin Hypercube method is used. The number of assessment samples are independent of the number of stochastic variables and depend on the type of the output parameter for the user. The high values of the system probability of failure lead to a low number of required MCS loops. In this research, 5000 replications have been utilized. It was assumed that the system probability of failure is due to the failure of each system component in terms of tensile, compressive, and deflection modes. For instance, whilst the inequation $GF_{S1}(\sigma) \prec 0$ is satisfied, it expresses that most probably, the tension failure will occur. The Monte-Carlo method is utilized due to calculating the probability of the failure. The performed calculations determine that the probable values of the failure or damage for the controlling-parameters are as follows: $p_f{}^{D} = 0$, $p_f{}^{t} = 1.55 \times 10^{-3}$, and $p_f{}^{C} = 0$. The safety index for the tensile stress limit state will be $\beta^{t} = 2.96$. Whereas the target safety index in the standard of ISO13822 offers a minimum value of 4.20. In some other research, the minimum value for the Trustworthy-Index for the bridge of the type in this research is suggested at values of 4.8 and 5.2 [34]. Due to the dissatisfaction of the target safety-index in the tensile stress failure function, the structure of the bridge is recognized as unsafe and is at risk of failure. In Figure 12, the values of the random samples show the maximum tensile stress occurring in the bridge, seen on the graph like a cloud (this figure is an example). For each sample in the case, the values of the actual tensile stress would be more than the allowed values, which will be considered as a failure event in the probability of failure.

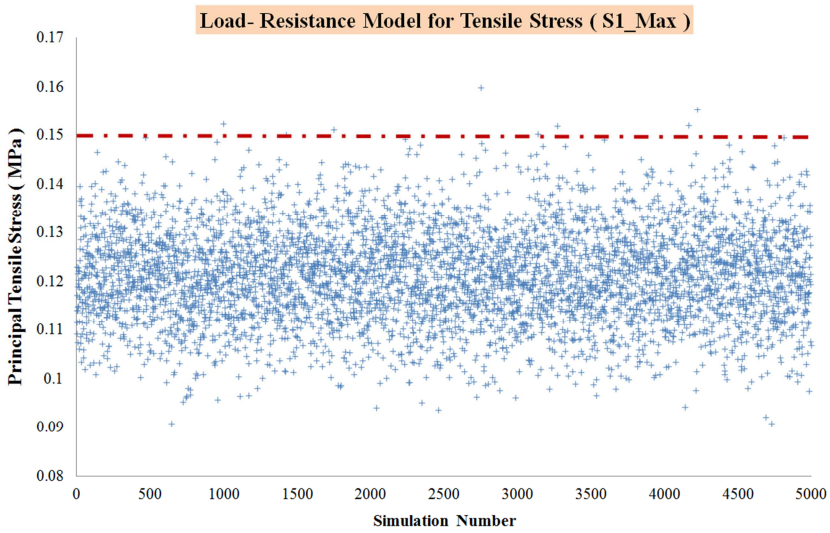

Fig. 12. Results history of Load–Resistance model of Tensile stress

The failure function for the tensile stress is shown by $GF_{S1}(\sigma)$. In the recently mentioned state, $GF_{S1}(\sigma) \prec 0$ and $I_C = 1$. In the case of each random sample, the failure function would be $GF_{S1}(\sigma) \succ 0$, and the value of I_c would be $I_C = 0$. In the general case, the system failure probability function will be calculated from Equations 4.1 to 4.5. In Equations 4.1 to 4.3, it is indicated how to determine the failure functions. In order to determine the failure functions of $GF_{LS}(X)$, we must subtract the critical exist values from their respective allowable values in every simulation loop, and if the values of the limit-state functions are negative, it indicates that the structural simulated model is unsafe, i.e. $GF_{LS}(X) \prec 0$; and if the value of the failure function is positive, it means the model is safe, i.e.

$GF_{LS}(X) \succ 0$.

$$GF_{S1}(\sigma) = S1^{allow} - S1^{\max}\ ;\ S1^{allow} = 0.15MPa \tag{4.1}$$

$$GF_{S3}(\sigma) = S3^{allow} - S3^{\min}\ ; S3^{allow} = 1.8MPa \tag{4.2}$$

$$GF_{Y}(D) = D^{allow} - D^{\max}\ ; D^{allow} = 5.75mm \tag{4.3}$$

$$P_f^{System} = P\left[P_f^{s3} \bigcup P_f^{s1} \cup P_f^{d}\right] = P[GF_{S3} < 0 \cup GF_{S1} < 0 \cup GF_{D} < 0] = 0 + P_f^{s1} + 0 \tag{4.4}$$

$$P_f^{System} = P_f^{S1} = \frac{\sum_{1}^{No.of\ .Sim.=5000} I_C}{No.of\ .Sim} \tag{4.5}$$

In Figure 13, the cumulative density functions (CDF) for the output parameters of deformation and stresses are shown. The cumulative functions for the output parameters of deflection and the stresses are shown in semi-logarithmic planes.

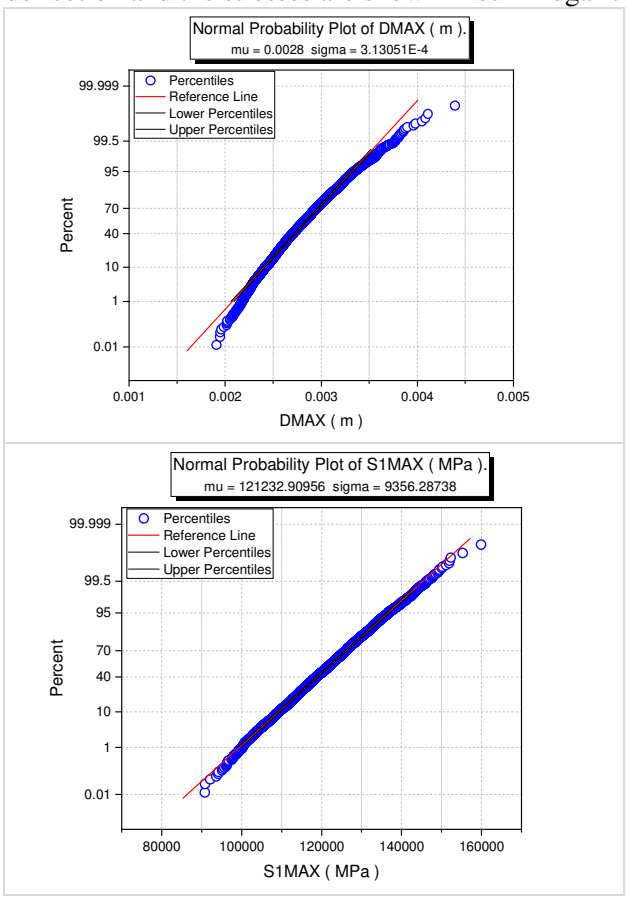

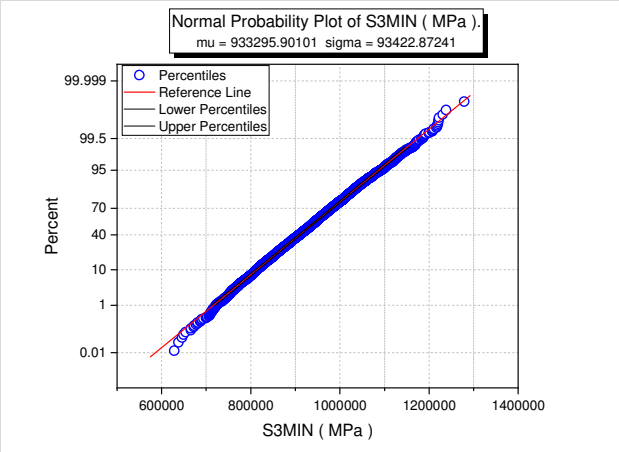

Fig. 13. The CDF for the output parameters

Equation 4.6 is utilized to calculate the safety-index (β_t). According to Equation (4.7), the safety-index should be greater than the target safety-index (β_t). The value of the target safety-index for historical structures of high importance is 4.2 [2,34]. In Excel software, the inversed CDF can be calculated with the following command: $\beta = -NORMSINV(p_f^{system})$. Figure 15 and Table 2 demonstrate the relationship between the reliability index and the safety factor of the BISTOON bridge. An increment in the safety factor would contribute to an improvement in the reliability index [30]. The segment between the values of 1.5 and 2, is quite steep.

$$\beta = -\Phi^{-1}(p_f^{system}) \tag{4.6}$$

$$\beta \geq \beta_t \tag{4.7}$$

Table 2. Safety Index of the BISTOON bridge for different Safety Factors

$L.S.$ / $Allow/Exist$	$S1_{Allow}$ (MPa)	$S3_{Allow}$ (MPa)	D_{Allow} (mm)	P_f	β
1	0.15	1.8	5.75	0.00154	2.96
1.5	0.225	2.7	8.625	0.00069	3.2
2	0.3	3.6	11.5	2.11E-06	4.6
2.5	0.375	4.5	14.375	9.96E-08	5.2
3	0.45	5.4	17.25	9.87E-10	6

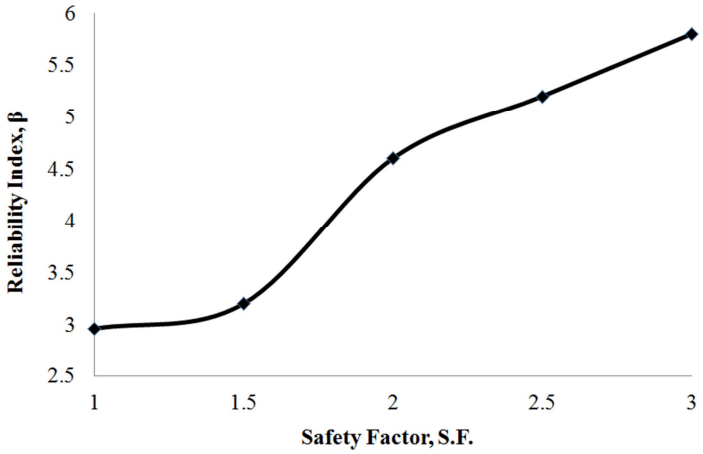

Fig. 14. Safety Index of BISTOON bridge for different Safety Factors

5. SENSITIVITY ANALYSIS

The analysis of the response of the structure with respect to the variation of the random variables in this section is explained. The standard pie-chart and bar-chart of the sensitivity analysis are given in detail in Figure 15. The maximum deflection limit function indicates that the maximum sensitivity is related to the variation of the modulus of elasticity of the vault and the lateral walls, and the minimum sensitivity is related to the modulus of elasticity of the infilled masonry and the bridge deck. For the limit function of maximum tensile stress, the maximum sensitivity is related to the variable of a specific mass of the infilled masonry and the deck materials and the minimum sensitivity is related to the modulus of elasticity of the infilled masonry and the deck materials. For the limit function of minimum compressive stress, the maximum sensitivity is related to the variable of the specific mass of the infilled masonry and the deck materials and the minimum sensitivity is related to the specific mass of the vault and the lateral walls. For all the cases in bar-charts, the negative values on the chart indicate the reverse effects of variables on the output parameters. For instance, by increasing the modulus of elasticity of the vault and the lateral walls, leads to decreasing the value of maximum deflection of the bridge. Similarly increasing the elasticity modulus of the infilled masonry and the deck materials leads to decreasing the maximum value of the bridge deflection. The correlation coefficient of the input variables with the output parameters checked in software results. It is obvious that there is not a specific correlation between the input variables, also between the output parameters of the bridge $(S1_{Allow}; S3_{Allow}; D_{Allow})$.

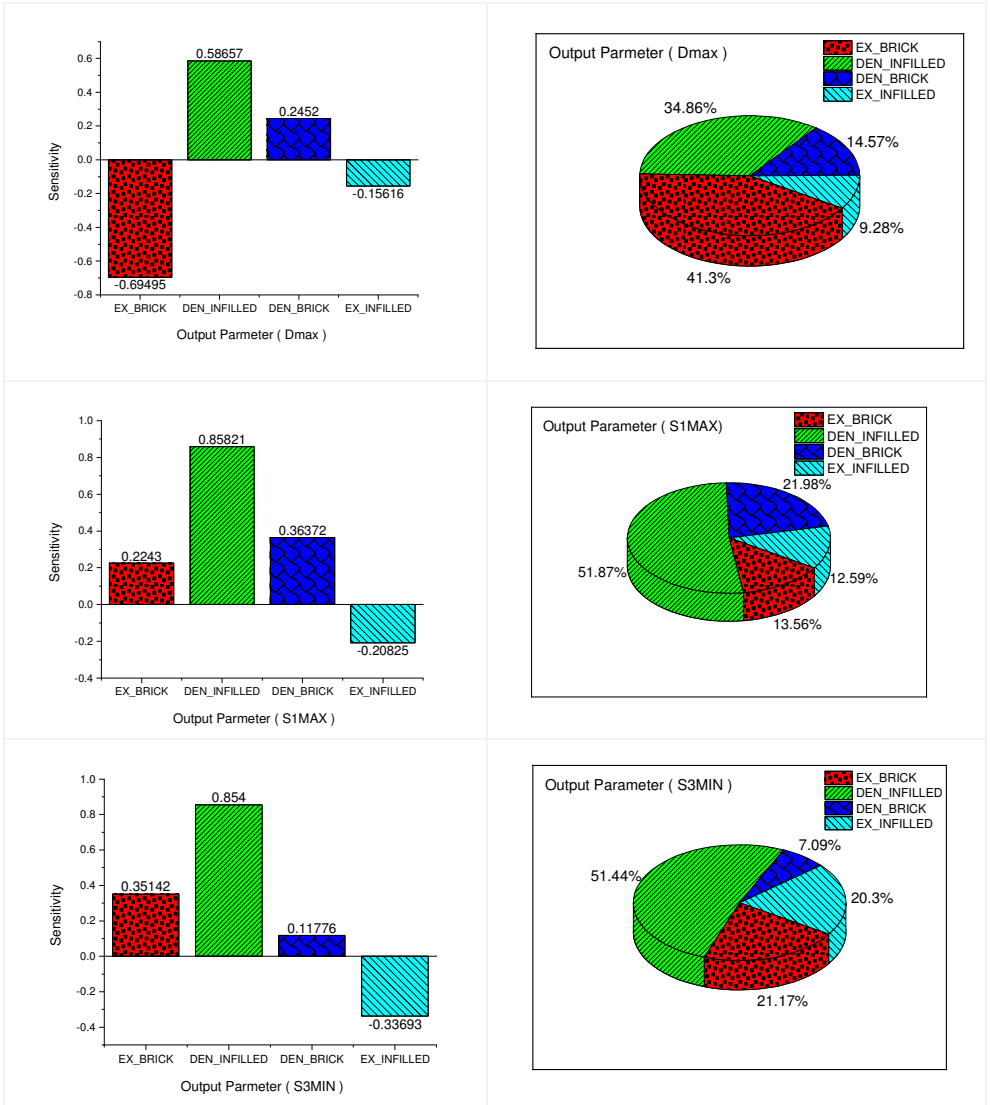

Fig. 15. Sensitivity analysis of the output parameters

6. CONCLUSION

In this research, the safety assessment of the masonry arch bridges with historical worth is evaluated with the case study of Bistoon arch bridge. Safety assessment solely performed under the serviceability of the bridge. The FEM has been conducted in the ANSYS software environment, where the capability of the parametric analysis is provided. As the structures of the cultural heritages are impressively worthy, thus they need to be analyzed precisely and accurately for their safety assessment. By assigning the variables of the modulus of elasticity, specific mass of the materials of bricks and infilled masonry materials, as random variable input parameters with uncertainties, the output parameters of the case of study will be evaluated. The output parameters include the maximum deflection of the bridge, the maximum tensile stress and the minimum compressive stress of the bridge. The output parameters are generated by the assumption of normal distribution and the coefficient of variation 10 percent and by 5000 loops. The Monte-Carlo method for the simulation and the Hypercube-Latin method for sampling has been utilized. Moreover, the sensitivity analysis to determine the sensitivity of the output parameters with respect to the variation of the input variables has been studied. It is concluded that the sensitivity of the rise of the bridge strongly depends on the variation of the infilled specific mass and modulus of elasticity of the masonry brick's material. Regarding the probability of failure with respect to the serviceability loads for the maximum-tensile stress limit state, it was determined that the bridge is prone to failure and unsafe, and the system failure probability is $p_f^{\ system} = 1.55 \times 10^{-3}$, where the equivalent safety index is $\beta^t = 2.96$; whilst the safety-index is lesser than the target safety index, i.e. $\beta^{T\arg et} = 4.2$. The required safety for the bridge has not been met and the bridge is at the risk of failure.

Conflict of Interest

The authors declare that they have no conflict of interest.

REFERENCES

1. Aliabdo, AAE and Elmoaty, AEMA 2012. Reliability of using nondestructive tests to estimate compressive strength of building stones and bricks. *Alexandria Engineering Journal* **51(3)**, 193-203.
2. Allen, DE 1992. Canadian highway bridge evaluation: reliability index. *Canadian Journal of Civil Engineering* **19(6)**, 987-991.

3. Altunişik, AC, Adanur, S, Genç, AF, Günaydin, M, and Okur, FY 2016. Non-destructive testing of an ancient masonry bastion. *Journal of Cultural Heritage* **22**, 1049-1054.
4. Altunışık, AC, Kanbur, B, and Genc, AF 2015. The effect of arch geometry on the structural behavior of masonry bridges. *Smart Struct. Syst* **16**(6), 1069-1089.
5. Asteris, PG, Moropoulou, A, Skentou, AD, Apostolopoulou, M, Mohebkhah, A, Cavaleri, L and Varum, H 2019. Stochastic Vulnerability Assessment of Masonry Structures: Concepts, Modeling, and Restoration Aspects. *Applied Sciences*, **9(2)**, 243.
6. Başbolat, EE, Bayraktar, A and Başağa HB (11-13 October 2018) *Seismic reliability analysis of high concrete arch dams under near-fault effect*, 4th International Conference on Earthquake Engineering and Seismology, TURKEY.
7. Beconcini, ML, Croce, P, Marsili, F, Muzzi, M and Rosso, E 2016. Probabilistic reliability assessment of a heritage structure under horizontal loads. *Probabilistic engineering mechanics* **45**, 198-211.
8. Bilgin, H and Huta, E 2018. Earthquake performance assessment of low and mid-rise buildings: Emphasis on URM buildings in Albania. *Earthquakes and Structures* **14(6)**, 599-614.
9. Borgna, G, Zanini, MA, Hofer, L, Faleschini, F and Matos, J 2019. *Structural Reliability of Masonry Arch Bridges Subject to Natural Aging*. In International Conference on Arch Bridges, Springer, Cham, October, 823-830.
10. Casas, JR 2011. Reliability-based assessment of masonry arch bridges. *Construction and Building Materials* **25(4)**, 1621-1631.
11. Del Monte, E, Boschi, S and Vignoli, A 2020. Prediction of compression strength of ancient mortars through in situ drilling resistance technique. *Construction and Building Materials* **237**, 117563.
12. Demircan, RK, Kaplan, G and Unay, AI 2019. *Determination of the Physical and Mechanical Properties of the Materials Used in The Northern City Walls of Historical Sinop Castle*. In IOP Conference Series: Materials Science and Engineering, IOP Publishing, February (Vol. 471, No. 8, p. 082039).
13. Dizhur, D, Lumantarna, R, Biggs, DT and Ingham, JM 2017. In-situ assessment of the physical and mechanical properties of vintage solid clay bricks. *Materials and Structures* **50(1)**, 63.
14. Domański, T and Matysek, P 2018. The reliability of masonry structures–evaluation methods for historical buildings. *Czasopismo Techniczne* **9**, 91108.

15. Ebrahimiyan, M, Golabchi, M and Yekrangnia, M 2017. Field Observation and Vulnerability Assessment of Gonbad-e Qābus. *Journal of Architectural Engineering* **23(4)**, 05017008.
16. Erkal, A and Ozhan, HO 2014. Value and vulnerability assessment of a historic tomb for conservation. *The Scientific World Journal*, 2014.
17. Fathi, A, Sadeghi, A, Emami Azadi, MR and Hoveidaie, N 2019. Assessing Seismic Behavior of a Masonry Historic Building considering Soil-Foundation-Structure Interaction (Case Study of Arge-Tabriz). *International Journal of Architectural Heritage*, 1-16.
18. Güllü, H and Jaf, HS 2016. Full 3D nonlinear time history analysis of dynamic soil–structure interaction for a historical masonry arch bridge. *Environmental Earth Sciences* **75(21)**, 1421.
19. Hacıefendioğlu, K, Başağa, HB and Banerjee, S 2017. Probabilistic analysis of historic masonry bridges to random ground motion by Monte Carlo Simulation using Response Surface Method. *Construction and Building Materials* **134**, 199-209.
20. Hradil, P, Žák, J, Novák, D and Lavický, M 2001. Stochastic analysis of historical masonry structures. Historical Constructions, PB Lourenço, P. Roca (Eds.).
21. Hariri-Ardebili, MA and Xu, J 2019. Efficient seismic reliability analysis of large-scale coupled systems including epistemic and aleatory uncertainties. *Soil Dynamics and Earthquake Engineering* **116**, 761-773.
22. Khaloo, A, Khoshnevis, A and Yekrangnia, M 2019. On the vulnerability of the Shrine of Prophet Daniel through field observation and numerical simulation. *Engineering Failure Analysis* **102**, 237-259.
23. Larsson, OSKAR 2015. Reliability analysis. Lecture notes, Lund University.
24. Mesquita, E, Arêde, A, Silva, R, Rocha, P, Gomes, A, Pinto, N and Varum, H 2017. Structural health monitoring of the retrofitting process, characterization and reliability analysis of a masonry heritage construction. *Journal of Civil Structural Health Monitoring* **7(3)**, 405-428.
25. Mesquita, E, Martini, R, Alves, A, Antunes, P and Varum, H 2018. Non-destructive characterization of ancient clay brick walls by indirect ultrasonic measurements. *Journal of Building Engineering* **19**, 172-180.
26. Micic, T and Asenov, M 2015. *Probabilistic model for ageing masonry walls*. In 12th International conferences on applications of statistics and probability in civil engineering, ICASP12, Vancouver, Canada.
27. Mishra, M, Bhatia, AS and Maity, D 2019. A comparative study of regression, neural network and neuro-fuzzy inference system for

determining the compressive strength of brick–mortar masonry by fusing nondestructive testing data. *Engineering with Computers*, 1-15.

28. Moreira, VN, Fernandes, J, Matos, JC and Oliveira, DV 2016. Reliability-based assessment of existing masonry arch railway bridges. *Construction and Building Materials* **115**, 544-554.
29. Moreira, VN, Matos, JC and Oliveira, DV 2017. Probabilistic-based assessment of a masonry arch bridge considering inferential procedures. *Engineering Structures* **134**, 61-73.
30. Muhammed, JJ 2019. Deterministic and Probabilistic Approaches in the Analysis of the Bearing Capacity of a Bridge Foundation on Undrained Clay Soil. *Slovak Journal of Civil Engineering* **27(2)**, 44-51.
31. Neiva, D, Moreira, VN, Matos, JC and Oliveira, DV 2017. *Robustness-based assessment of railway masonry arch bridges*. International Association for Bridge and Structural Engineering. In IABSE Symposium Report, September, Vol. 109, No. 16, 2840-2847.
32. Noor-E-Khuda, S and Albermani, F 2019. Mechanical properties of clay masonry units: Destructive and ultrasonic testing. *Construction and Building Materials* **219**, 111-120.
33. Pouraminian, M, Pourbakhshian, S, Farsangi, EN and Fotoukian, R 2019. Probabilistic safety evaluation of a concrete arch dam based on finite element modeling and a reliability IR approach. *Civil and Environmental Engineering Reports* **4(29)**, 062-078.
34. Pouraminian, M, Pourbakhshian, S and Hosseini, M 2019. Reliability analysis of Pole Kheshti historical arch bridge under service loads using SFEM. *Journal of Building Pathology and Rehabilitation* **4(1)**, 21.
35. Pouraminian, M, Sadeghi, A and Pourbakhshiyan, S 2014. Seismic behavior of Persian brick arches. *Indian Journal of Science and Technology* **7(4)**, 497.
36. Pourbakhshian, S and Ghaemain, M 2016. Shape optimization of arch dams using sensitivity analysis. *KSCE Journal of Civil Engineering* **20(5)**, 1966-1976.
37. Reh, S, Beley, JD, Mukherjee, S and Khor, EH 2006. Probabilistic finite element analysis using ANSYS. *Structural Safety* **28(1-2)**, 17-43.
38. Sadeghi, ARJANG and Pouraminian, M 2010. *An investigation of the vulnerability of Arge Tabriz (Tabriz Citadel)*. In 8th International Masonry Conference in Dresden, July.
39. Silveira, D, Varum, H, Costa, A, Martins, T, Pereira, H and Almeida, J 2012. Mechanical properties of adobe bricks in ancient constructions. *Construction and Building Materials* **28(1)**, 36-44.

40. Valluzzi, MR, Lorenzoni, F, Deiana, R, Taffarel, S and Modena, C 2019. Non-destructive investigations for the structural qualification of the Sarno Baths, Pompeii. *Journal of Cultural Heritage* **40**, 280-287.

Editor received the manuscript: 08.02.2020